The effects of clipped photon detection in speckle interferometry and speckle masking techniques[*]

E. Aristidi and C. Aime

Département d'Astrophysique de l'Université de Nice – Sophia Antipolis, U.R.A. 709 du C.N.R.S., Parc Valrose, 06108 Nice Cedex 2, France

November 14, 1995

Abstract. This paper present numerical illustrations of the effects of clipping of photoevents in speckle interferometry and speckle masking. The clipping is due to a saturation of the photon-counting detectors that cannot count more than one photon per pixel, causing the image to be composed of "0" and "1". The theoretical basis for this study has been published by Aime and Aristidi (1992). Clipping effects are investigated numerically on real star data. As predicted by theory, the clipping introduces several effects on auto and triple correlation functions, such as a linear global loss of energy, and non linear terms which affects mainly the high frequencies. Attention is focused on the way the astronomical information is affected by this kind of detection, especially for the case of the double stars.

1. Introduction

Observation of weak sources in speckle interferometry requires the use of fast photon-counting cameras. Photons can be detected one by one as they arrive, with their spatial coordinates and arrival time ; this is the case with, for example, the PAPA camera (Papaliolios et al. 1985). The detection can be performed as well frame by frame, a single frame being the result of an integration of a few milliseconds ; intensified CCDs like CP40 (Blazit 1987) belong to this later class of device. Features of these detectors are the large number of pixels and the excellent stability of the CCDs.

Because the detectors are not perfect, the photon images suffer from various artifacts, such as geometric distorsions or the well-known "photon counting hole" caused by the centroiding electronics (Blazit et al. 1975). A review of these problems has been made by Foy (1987). Hoffmann

(1993) makes a description of possible solutions to the photon counting hole problem. A more recent paper relative to this subject has been written by Thiebaud (1994).

The problem we shall examine is somewhat different to that of the photon counting hole, but appears for similar reasons. It is the so-called "clipping" effect of photoevents ; clipping denotes the effect of a saturation of the device that does not allow the detector to differentiate between a single photon and more than one photon. Clipping basically affects photon cameras of the integration type, but is also likely to influence sequential ones if possible dead-time reactions are to be considered.

In practice, these effects are generally neglected owing to the very low probability of occurence of more than one photon per pixel for the weak astronomical sources of interest, giving generally less than one hundred photons per image. Moreover, these experimental approximations might appear, at a first glance, to be well supported by the theoretical approach that describes the photon noise limitation in speckle interferometry as a compound Poisson impulse process, where it is assumed that the probability of more than one photoevent is vanishingly small compared with the probability of one or zero photoevents. Then the signal is modelized as a sum of unit impulses at different spatial locations. As emphasized by Goodman (Goodman 1985), this representation assumes that the detector is continuous in space. Taking into account the finite dimensions of the pixels of the detectors, the ideal distribution is integrated and leads directly to Poisson statistics for the number of photons occuring in a fixed pixel size. The ideal photodetected image is given by the number of photons (theoretically from 0 to ∞) occuring in each pixel. The effect of clipping acts on the saturation of the Poisson law for each pixel.

A technique of clipping is sometimes used in the field of laser optics where it is applied as a tool for data compression. A few papers deal with the effects of clipping on speckle interferograms at high light level (Marron & Morris 1985; Ohtsubo & Ogirawa 1988; Pedersen 1984).

---

[*]: Based on observations collected at the 1.93m of the Observatoire de Haute Provence, France

The case of photon-counting detection has been studied by Barakat (1988) who gives the expression of the autocorrelation function (AC) for a point source fully developed speckle pattern.

In high angular resolution astronomical imaging, the information destroyed by the atmospherical turbulence, can be partly recovered by means of statistical functions of the random instantaneous images, as first shown by Labeyrie in the early 70's (Labeyrie 1970). The AC of the images can give, for example, the angular separation of a very close double star. The triple correlation (TC) can be used to recover a diffraction-limited image of the observed object (Weigelt 1991). Clipping affects these statistical functions and destroy the linear object-image convolution relation. A general study has been published recently (Aime & Aristidi 1992) and mathematical expressions were given for the clipped AC and TC ; this paper will be referenced in this text as Paper I. Other partial results on clipping and parts of the present paper can be found in Aime et al. (1990), Aime et al. (1991), Aristidi at al. (1991).

The photodetected AC and TC suffer from an important bias due to the statistics of the photons. Petrov et al. (1982) have proposed a technique based on a simultaneous double detection of the photon-counting speckle patterns ; the bias disappear if one computes, instead of the AC, the cross correlation between the two detections of each image. Some astrophysical results using this technique can be found in the paper of Thiebaud (1994). These have been generalized to the TC by Hoffman and Weigelt (1987) using three simultaneous detections of each image. Cross AC/TC will be taken into account in our presentation. Nevertheless these functions will be referenced as AC and TC in the text.

Our present paper is basically a numerical illustration of Paper I, as announced at the end of it. General relations of Paper I are summarized in section 2. Section 3 gives some numerical illustrations of single and double stars speckle patterns under different clipping conditions. In addition to the mathematical expressions valid for a fully developped speckle pattern, we have made use of speckle interferograms of the star Vega in the visible. A discussion of the results is given in section 4.

2. General expressions for clipped AC and TC functions

This section is devoted to a brief summary of the basic equations as derived in Aime and Aristidi (1992). These equations are valid for spatially stationnary speckle patterns. The main point is that single photon-clipped AC and TC can be expressed as functions of the multifold PDF of the event "0 photon" of a perfectly photodetected image. This later quantity can be directly derived from the high light level probability density function (PDF) of the speckle pattern. The presentation we give here has been somewhat simplified with regard to that of Paper I.

We use the following notations :

- $I(\mathbf{r})$ denotes the classical integrated intensity falling on a pixel at position $\mathbf{r}$, $I_p(\mathbf{r})$ is the photon-limited image that could be given by a perfect photon camera and $I_c(\mathbf{r})$ is the single photon clipped image made of a succession of "0" and "1" where the value "1" is registred for one or more incident photons.
- $\bar{n}$ is the mean number of photon per pixel in $I_p(\mathbf{r})$.
- $C(\rho)$, $C_p(\rho)$ and $C_c(\rho)$ are the AC of $I(\mathbf{r})$, $I_p(\mathbf{r})$ and $I_c(\mathbf{r})$ respectively ; ρ beeing here the spatial lag vector.
- $T(\rho_1, \rho_2)$, $T_p(\rho_1, \rho_2)$ and $T_c(\rho_1, \rho_2)$ are the TC of $I(\mathbf{r})$, $I_p(\mathbf{r})$ and $I_c(\mathbf{r})$ respectively ; ρ_1 and ρ_2 are the spatial lags.

For a single photon clipped image, the possible events are of the form of Bernouilli trials. Let us denote as η_i the random variable equal to 1 when one (ore more) photons are detected i pixel i and 0 otherwise, and ξ_i the random variable associated with the contrary event ; ξ_i is equal to 1 for no photon detected in pixel i, and 0 otherwise. By definition we have :

$$\eta_i + \xi_i = 1 \qquad (1)$$

The mean number of detected photons per pixel of the clipped image can be expressed as :

$$m_c = E[\eta_i] = E[1 - \xi_i] = 1 - E[\xi_i] = 1 - p_1(0) \qquad (2)$$

where $E[...]$ denotes the expected value. We have assumed space stationnarity by writing that $E[\xi_i]$ is independent of the spatial position i. The quantity $p_1(0)$ represent the probability of the event "0 photon" in a pixel. Since this quantity is not affected by the clipping process, $p_1(0)$ is also the value of $p_1(n)$ (the probability of detecting n photons in a pixel for a perfect photodetected image) for $n = 0$. This approach can be generalized staightforwardly to the computation of clipped AC and TC. We have :

$$C_c(\rho) = E[\eta_i \eta_j] = E[(1 - \xi_i)(1 - \xi_j)]$$
$$= 1 - E[\xi_i] - E[\xi_j] + E[\xi_i \xi_j] \qquad (3)$$

It is necessary to consider the two cases $\rho = 0$ and $\rho \neq 0$. For $\rho = 0$, i.e. $i = j$, the product $\xi_i \xi_j$ is equal to ξ_i^2. With the 0–1 definition of ξ_i, we can write $\xi_i^2 = \xi_i$, and the value of $C_c(0)$ reduces to m_c. For $\rho \neq 0$ and assuming space stationnarity, $E[\xi_i \xi_j]$ can be written as $p_2(0, 0; \rho)$, the probability of the joint occurence of the events 0 photon for two pixels distant ρ. The overall clipped AC becomes :

$\bullet$ $C_c(0) = 1 - p_1(0)$

$\bullet$ $C_c(\rho \neq 0) = 1 - 2p_1(0) + p_2(0, 0; \rho)$

$$(4)$$

Similarly, the TC of the clipped image can be written as :

$$T_c(\rho_1, \rho_2) = E[\eta_i \eta_j \eta_k] = E[(1 - \xi_i)(1 - \xi_j)(1 - \xi_k)]$$

$$= 1 - E[\xi_i] - E[\xi_j] - E[\xi_k] + E[\xi_i \xi_j] \quad (5)$$

$$+ E[\xi_i \xi_k] + E[\xi_j \xi_k] - E[\xi_i \xi_j \xi_k]$$

Here again we must take into account the particular values $\rho_1 = 0$ and/or $\rho_2 = 0$ that make some of the spatial positions i, j and k identical. We obtain :

- $T_c(0,0) \quad = 1 - p_1(0) = C_c(0)$

- $T_c(\rho_1, 0) \quad = 1 - 2p_1(0) + p_2(0,0;\rho_1) = C_c(\rho_1)$

- $T_c(0, \rho_2) \quad = 1 - 2p_1(0) + p_2(0,0;\rho_2) = C_c(\rho_2)$

- $T_c(\rho_1, \rho_1) = 1 - 2p_1(0) + p_2(0,0;\rho_1) = C_c(\rho_1)$ (6)

- $T_c(\rho_1, \rho_2) = 1 - 3p_1(0) + p_2(0,0;\rho_1) + p_2(0,0;\rho_2)$

$$+ p_2(0,0;\rho_2 - \rho_1) - p_3(0,0,0;\rho_1,\rho_2)$$

where $p_3(n_1, n_2, n_3; \rho_1, \rho_2)$ is the three-fold PDF of the perfect photodetected image, $p_3(0,0,0;\rho_1,\rho_2)$ being the probability of the event "0 photon" for three different pixels ρ_1 and ρ_2 distant.

Since the variance of the photons affects only the origin of the AC/TC, cross-correlations may be obtained by using the general term of equations 4 and 6 for $\rho = 0$, $\rho_1 = 0$ and $\rho_2 = 0$. All the results presented in this paper as AC/TC are in fact cross-correlations.

Now we need to express $p_1(0)$, $p_2(0,0;\rho)$ and $p_3(0,0,0;\rho_1,\rho_2)$. These quantities may be derived from the statistics of the high light level images. Indeed, high-light level and photon counting PDF's are related one another by the Poisson Transform (Goodman 1985). For the singlefold PDF, we have :

$$p_1(n) = \int_0^\infty \frac{(\alpha\Omega)^n}{n!} e^{-\alpha\Omega} P_1(\Omega) \, d\Omega \quad (7)$$

where $P_1(\Omega)$ is the PDF of the perfect intensity image and $\alpha = E[n]/E[\Omega]$ the quantum efficiency of the detector. We just need to compute this expression for $n = 0$ and the above relation can be resumed to :

$$p_1(0) = \int_0^\infty e^{-\alpha\Omega} P_1(\Omega) \, d\Omega \quad (8)$$

The calculation generalizes easily to two and three dimensions :

- $p_2(0,0;\rho) = \iint e^{-\alpha(\Omega_1 + \Omega_2)} P_2(\Omega_1, \Omega_2; \rho) \, d\Omega_1 \, d\Omega_2$

- $p_3(0,0,0;\rho_1,\rho_2) = \iiint e^{-\alpha(\Omega_1 + \Omega_2 + \Omega_3)}$ (9)

$$\times P_3(\Omega_1, \Omega_2, \Omega_3; \rho_1, \rho_2) \, d\Omega_1 \, d\Omega_2 \, d\Omega_3$$

where P_2 and P_3 are the two- and three-fold PDF's of the speckle images.

At very low light levels, $\alpha\Omega \ll 1$, and one can develop the exponential terms into a power expansion ; equations 4 and 6 lead to the following approximations :

$$C_c(\rho) = C_p(\rho) - \frac{\alpha^3}{2} \left(T(0,\rho) + T(\rho,\rho) \right) + \frac{\alpha^4}{12} \left(2Q(0,0,\rho) \right.$$

$$\left. + 3Q(0,\rho,0) + 2Q(\rho,0,0) \right) + o(\alpha^4) \quad (10)$$

$$T_c(\rho_1, \rho_2) = T_p(\rho_1, \rho_2) - \frac{\alpha^4}{2} \left(Q(\rho_1,\rho_2,0) + Q(\rho_1,\rho_2,\rho_1) \right.$$

$$\left. + Q(\rho_1,\rho_2,\rho_2) \right) + o(\alpha^4) \quad (11)$$

Where $Q(\rho_1, \rho_2, \rho_3)$ is the fourth-order correlation of the high-light images. The clipping may be considered as a first approximation in a mixing between statistical functions of different orders. These equations may be used for an easy computation of the clipped AC/TC at low light level (typically under 0.01 photon/pixel). A comparison between the different approximation orders of the clipped AC is shown in fig. 4.

At that level, we have used two approaches to obtain a quantitative estimate of the effects of the clipping on AC and TC. The first one is based on the use of real data to compute high-light level PDF's. The second one is fully theoretical and assumes that the complex amplitude of the point source speckle pattern is a circular gaussian random variable.

2.1. Use of real data to simulate clipped AC and TC

The data material consist of speckle interferograms obtained at the 193 cm telescope of the Observatoire de Haute Provence, France, on an unresolved star (Vega). The telescope was used in Cassegrain configuration (focal length of 30 m) with a ×15 microscope objective and a red filter. The images were captured using an intensified video CCD camera. The exposure time was 20 ms for each frame. An example of such images is shown in fig. 2. Altogether 1200 images were recorded and processed. We denote as $V(\mathbf{r})$ these images.

The simulation of speckle patterns corresponding to the observations of a double star, or of a structured object, was obtained by convolving each individual image with the intensity distribution of the desired object, owing to the object-image convolution relation valid in the isoplanetism domain (Labeyrie 1970). To make a complete description of a double star having an intensity ratio β and a separation vector $\mathbf{d}$, one can simply write the quantity $V(\mathbf{r}) + \alpha V(\mathbf{r} - \mathbf{d})$ for each instantaneous frame.

The clipped AC/TC were computed using eqs. 4 and 6 ; the quantities $p_1(0)$ and $p_2(0,0;\rho)$ are estimated as follows :
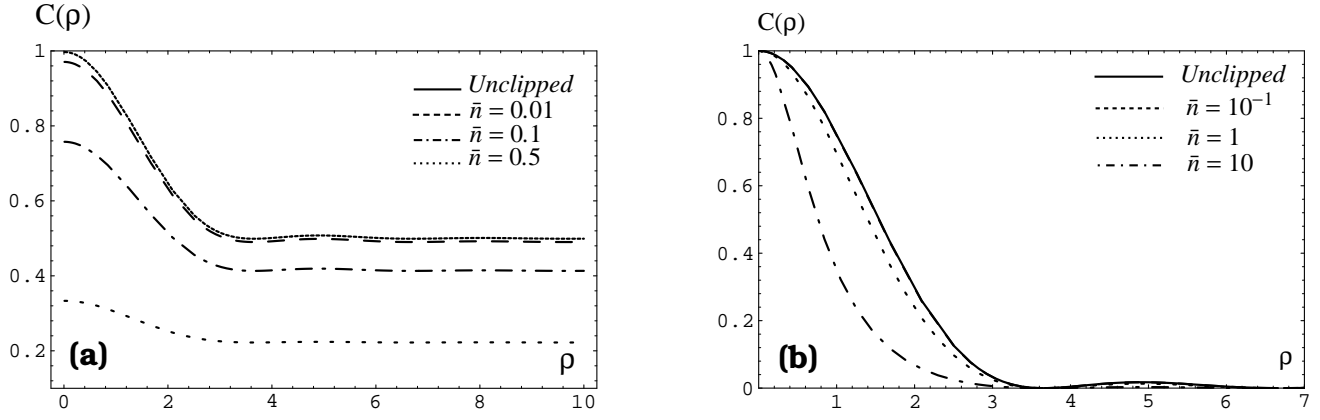
Fig. 1. Graphs of the autocorrelation functions of fully developped point-source speckle patterns computed using eq. 4 with a coherence factor $r(\rho) = 2\frac{J_1(\Pi\rho/s)}{\pi\rho/s}$, corresponding to a circular aperture telescope, s being the size of the speckle. (a) plots of the ratio $C_c(\rho)/C(0)$ for several values of the mean number of photon per pixel $\bar{n}$. These curves show the influence of the multiplicative factor Λ defined in relation 13. Note that : (i) the effect is neglectible for $\bar{n}$ smaller than 10^{-2} where $\Lambda = 0.98$ and (ii) the attenuation affects mainly the small values of the spatial lag ρ, i.e. near $r(\rho)$=1, due to the $r^2(\rho)$ dependency in the power expansion of Λ (see relation 13). (b) The same functions drawn between their respective minimum and maximum ; this is to put in evidence the "super-resolution" non-linear effect caused by the clipping. It is quite insensible for $\bar{n}$ smaller than 0.1.

1. Bin the intensity value of the synthesized speckle pattern over 64 integer values.
2. Compute the histogram and joint-occurrence histograms of the binned images. Normalise them so that their integral is 1. Because of the binning procedure, the mean m is of a few tenths of units.
3. Allow the parameter α to vary so that the average number of photon $\bar{n}$ takes the required value. Compute the quantities $p_1(0)$, $p_2(0,0;\rho)$ and $p_3(0,0,0;\rho_1,\rho_2)$ using relations 8 and 9 (Poisson transforms of the above joint occurence histograms).

We would like to point out that this approach is not a complete simulation since we do not start from images of photon impacts. However the advantage of our method is triple. First, it allows us to compute the AC/TC for several values of the average number of photons per pixel from one set of intensity PDF's, by adjusting the parameter α to a relevant value. Second, it is easy to compute cross-correlations, while in a complete simulation one would generate two photon-counting images by individual intensity pattern. The third advantage is that the SNR of the power spectrum obtained by this procedure is that of the high-light level images.

2.2. Analytical expressions for the Gaussian case

For a fully developped speckle pattern , i.e. when the complex amplitude of the wave at the focus of the telescope is a Gaussian circular random variable, analytical expressions are available for $p_1(0)$, $p_2(0,0;\rho)$ and $p_3(0,0,0;\rho_1,\rho_2)$.
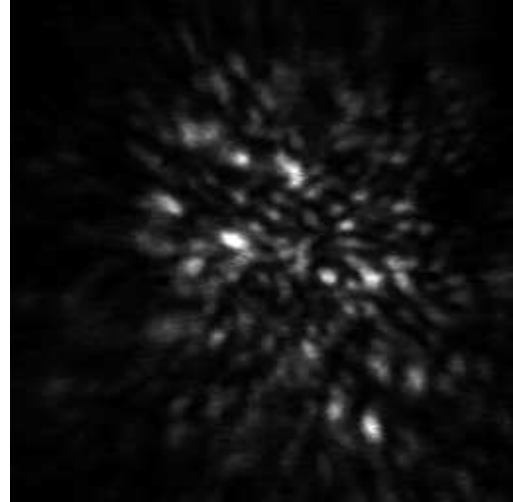
Fig. 2. Typical speckle interferograms of the star Vega (α Lyr) observed at the 193 cm OHP telescope (the field of the image is 2.9 arcsec and the value of r_0 is about 7 cm).

For the point source the expressions of the probabilities p_1, p_2 and p_3 are :

$$\bullet\, p_1(0) = \frac{1}{1+\bar{n}}$$

$$\bullet\, p_2(0,0;\rho) = \frac{1}{1 + 2\bar{n} + \bar{n}^2(1 - r^2(\rho))}$$

$$\bullet\, p_3(0,0,0;\rho_1,\rho_2) = [(1+\bar{n})^3$$

$$-\bar{n}^2(r^2(\rho_1) + r^2(\rho_2) + r^2(\rho_2 - \rho_1))$$

$$+ 2\bar{n}^3 r(\rho_1)r(\rho_2)r(\rho_2 - \rho_1)]^{-1}$$

(12)

where $r(\rho)$ is the correlation function of the complex amplitude for two points distant ρ of the incident wave. $r(\rho)$ gives an idea of the spatial extension of the shape of the speckles. It contains in particular the pupil of the telescope (Goodman 1985). The demonstration of above relation is very briefly given in the appendix.

3. Results

3.1. For the point-source

The study of the point source can provide interesting informations upon the modifications that may occur on the AC and the TC through the clipping process.

3.1.1. On the AC

One can distinguish between two effects :

The first one is a linear multiplicative coefficient Λ which weakens all the values of the AC. This attenuation is visible on theoretical curves valid for the Gaussian model (fig. 1a) as well as on the images of Vega (fig. 3a). The clipped AC can be written combining eqs. 4 and 12 :

$$C_c(\rho) = 1 - \frac{2}{1+\bar{n}} + \frac{1}{1+2\bar{n}+\bar{n}^2(1-r^2(\rho))} \quad (13)$$

The coefficient Λ is defined as the ratio of clipped to unclipped AC and is constant at the first order in $r(\rho)$; the expression of the unclipped AC has been given by Goodman (1985) : $C_p(\rho) = \bar{n}^2(1+r^2(\rho))$.

$$\Lambda = \frac{C_c(\rho)}{C_p(\rho)} = \frac{1+\bar{n}(1-r^2(\rho))/(1+r^2(\rho))}{1+\bar{n}\left[3+\bar{n}(3-r^2(\rho))+\bar{n}^2(1-r^2(\rho))\right]} \quad (14)$$

which can be approximated when α is small by :

$$\Lambda \simeq \frac{1}{(1+\bar{n})^2} \quad (15)$$

As expected, Λ goes fainter as $\bar{n}$ increases ; it tends towards 1 when $\bar{n} \to 0$ which is not surprising owing the very low probability of the occurence of two simultaned photoevents in that case. In the asymptotic case where $\alpha \to \infty$, all the pixels of the image become saturated and the AC tends towards a constant (since space stationnarity is assumed througout this paper).

Equation 10 gives an approximation of the clipped AC for small values of $\bar{n}$: it is equal to the unclipped AC plus correcting terms of higher statistical order. The two first correcting terms (triple correlation and quadricorrelation), given in eq. 10, are plotted in figure 4a for $\bar{n} = 0.1$. The two first correcting terms give a good approximation of the clipped AC at this level of light. Curves 4b are the corresponding transfer function, but for $\bar{n} = 1$. They were normalized between 0 and 1 in order to put in evidence the non linear effect. They show that this effect is not represented by the first two correcting terms, which is not very

surprising because either the bispectrum and the Fourier transform of the quadricorrelation are spatially limited by the cutoff frequency of the telescope.

The second effect appears only when the number of photon per pixel is high ($\bar{n} > 0.1$) and can be interpreted as an asymptotic behaviour with no real application to astronomy. It consists in a slight modification of the AC s curve shape : the width of the central peak decreases as α increases. This is clearly visible on the analytical curves (fig. 1b) but not on the AC of Vega (fig. 3b). The corresponding transfer functions are plotted in fig. 5 ; part of the energy is spread beyond the cutoff frequency of the telescope. This effect may be understood as the signature of the higher orders statistical terms that appear in the AC when the clipping occurs.
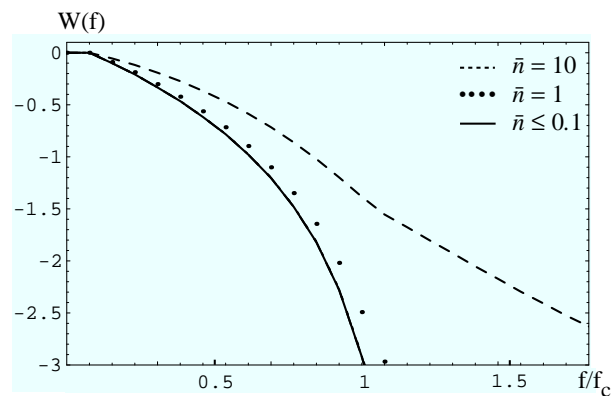
Fig. 5. Clipped transfer functions calculated with the theoretical model. The parameters of the computation are the same than those of figure 1. When $\bar{n} > 0.1$ photon per pixel, some energy is spread beyond the theoretical telescope cutoff frequency f_c.

3.1.2. On the TC

The effects are qualitatively the same for the AC and for the TC : a global loss of energy, and non-linear effect of contration of the central peak of the point-spread TC.

Regarding to the linear effect, we can define a coefficient Λ' as the ratio of clipped to unclipped TC ; the expressions of the clipped TC are deduced from eqs. 6 and 12. For small values of α it apprxoximates to :

$$\Lambda' \simeq \frac{1}{(1+\bar{n})^3} \quad (16)$$

An illustration can be found in fig 6. The TC is normally a fourth dimensionnal function of the vectors spatial lags ρ_1 and ρ_2, these vectors have been taken aligned so that the TC becomes two dimensionnal. A one-dimensionnal cut along the second bissector ($\rho_2 = -\rho_1$),
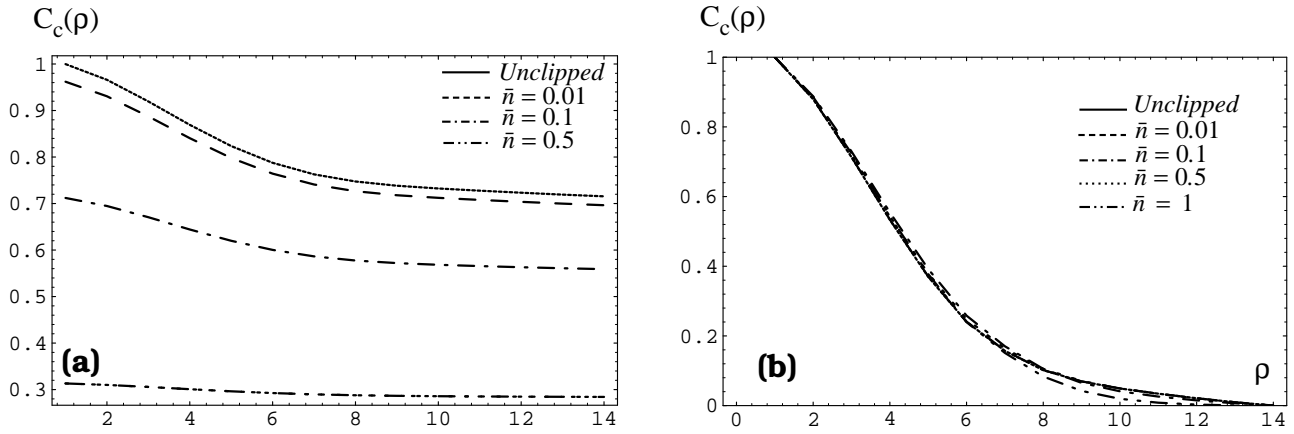
Fig. 3. Graphs of the clipped autocorrelation functions calculated from 1200 hight-light images of Vega using the procedure descibed in section 2.1. (a) Drawn to scale for different values of $\bar{n}$, the curves show the linear multiplicative coefficient Λ defined in the text. The behavior of these simulated AC appears to be in good agreement with the theoretical model (see figure 1). (b) The same curves are drawn between their respective maximum and minimum, in order to put in evidence the non-linear effect of narrowing of the peak of the AC ; this effect is almost negligible here, but one must keep in mind that the dynamic of the AC becomes very small where $\bar{n}$ increases. As a consequence we can expect that the non-linear effect is very difficult to see on real data.
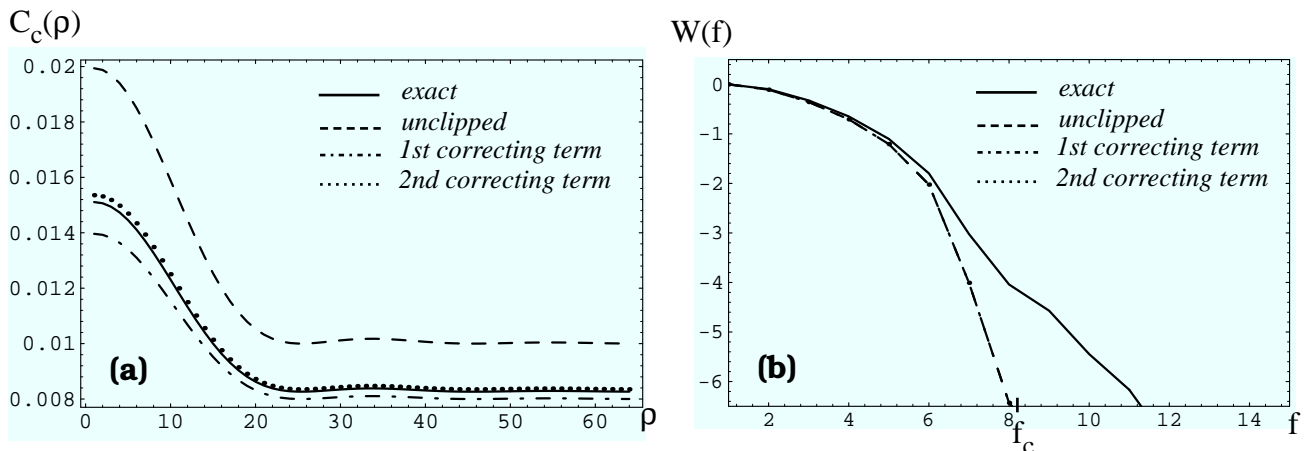
Fig. 4. Illustrations of eq. 10. (a) Graphs of the clipped AC of the PSF of a circular aperture telescope, for $\bar{n} = 0.1$ photon/pixel. The full line is the exact calculation and the dashed lines are the three different levels of approximation appearing in eq. 10, i.e. the unclipped AC, the unclipped AC plus the first term in triple correlation, and the unclipped AC plus the two first terms. (b) Graphs of the transfer functions but for a higher level of light ($\bar{n} = 1$ ph/pix). The functions are normalized between 0 and 1 in order to put in evidence the non-linear effect. All the curves are identical excepted the exact one showing an extension after the cutoff frequency referenced by f_c on the graph

plot on fig 6b shows the effect of Λ'. Note that the attenuation is worse for the TC than for the AC, according to the term in $(1 + \bar{n})^{-3}$ for the TC, against the one in $(1 + \bar{n})^{-2}$ for the AC.

The nonlinear effect has been also investigated on the TC. We show on figure 7 the FWHM of the point-spread AC and TC, as a function of the mean number of photon per pixel $\bar{n}$. These curves have been calculated using the analytical model with $r(\rho) = \exp(-\rho^2/s^2)$. It appears

that this effect may be neglected for $\bar{n} < 0.01$ where the FWHM of the clipped AC/TC differs from less that 1% from the unclipped functions. Note the strange behavior of the FWHM of the TC, which present a bump near $\bar{n} = 0.1$. The TC is less sensitive to the clipping than the AC in the high light level range, while the AC gives more accurate results around 0.1 photon per pixel.
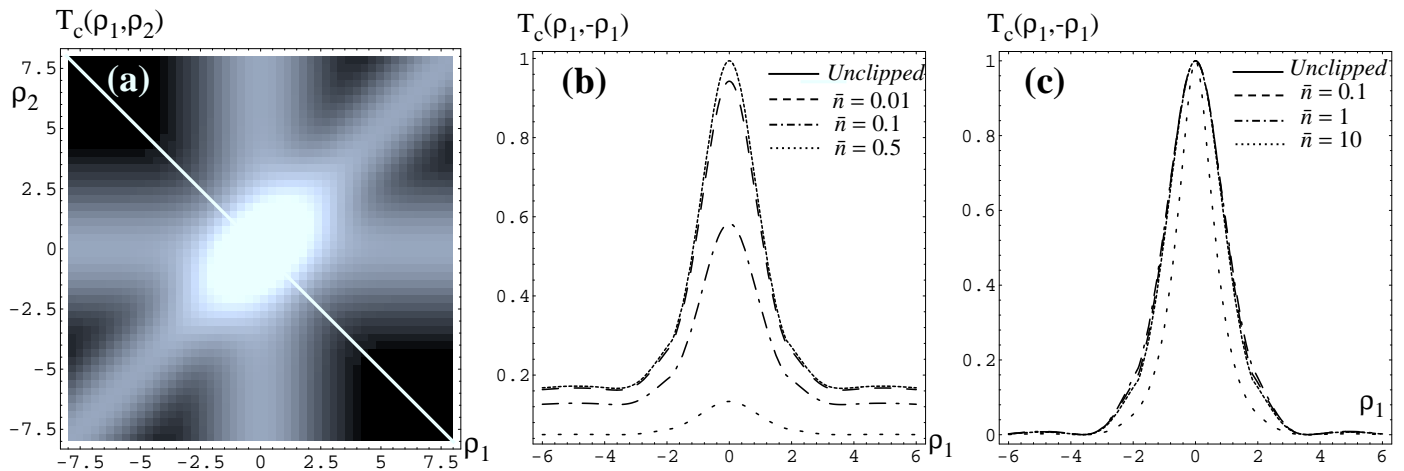
Fig. 6. Illustration of the clipping on the TC of a point-source speckle pattern calculated analytically from eqs. 6 and 12 with the same coherence factor $r(\rho)$ than fig. 2. (a) the two-dimensionnal plot of $T_c(\rho_1, \rho_2)$; the blanck line is the direction $(\rho_2 = -\rho_1)$ along which are calculated the curves (b) the influence of the multiplicative factor Λ' and (c) the effect of contraction of the pincipal peak. (Curves normalized between their maximum and minimum)
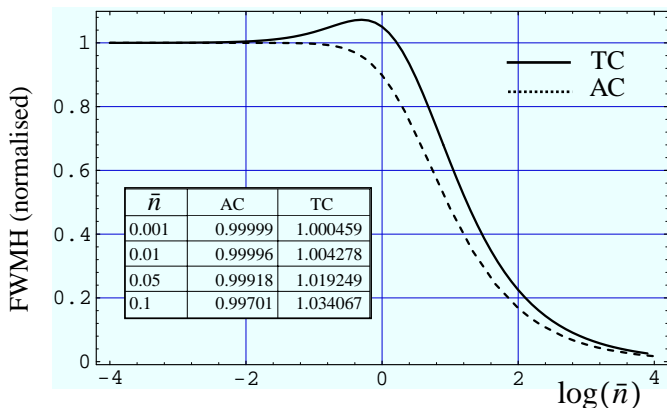
Fig. 7. Plot of the FWHM of the peak of the clipped AC (dashed line) and TC (full line), as a function of $\bar{n}$. For the TC the calculation has been made along the second bissector $(\rho2 = -\rho_1)$. The curves have been computed with the analytical model, with $r(\rho) = \exp(-r^2/s^2)$, (s is the size of the speckle). They have been normalised to the FWHM of the unclipped functions.

3.2. Visibility functions of a resolved star

Among the astronomical objects frequently observed in speckle interferometry, one finds the giant stars close enough to be resolved by the large telescopes or by the interferometers (Foy 1991; Quirrenbach 1991). This section will present by means of simulation the effects of the clipping on the visibility functions of a giant star modelled by an uniform disc.

The visibility function $V(f)$ of an object is defined by the ratio of the power spectrum of speckle interferograms of the object, to the power spectrum estimated on a close reference star. The object-image convolution relation (Roddier 1988) predicts that $V(f)$ identifies to the square modulus of the Fourier transform of the object, an Airy function in our case.

The calculation was made as follows :

- Simulation of 1000 speckle interferograms corresponding to a 2 m circular aperture telescope operated at a wavelength of 5000 Å, and a turbulence characterized by a Fried parameter $r_0 = 20$ cm.
- Computation of the clipped power spectrum $W_p(f)$ for a mean number of photon per pixel $\bar{n}_p$.
- Convolution of all the speckle patterns by an uniform disc of diameter 6 pixels
- Computation of the clipped power spectrum $W_o(f)$ for a mean number of photon per pixel $\bar{n}_o$.
- Calculation of the visibility function $V(f) = \frac{W_o(f)}{W_p(f)}$.

The clipping occurs here at two levels, affecting both the power spectrum of the object and of its reference. Very often the reference star is choosen brighter than the object for SNR reasons ; in such a case the clipping effects are not the same on both cases.

The results of the simulation are presented in figure 8. Several visibility functions have been calculated for various values of $\bar{n}_p$ and $\bar{n}_o$ varying between 0.001 and 0.1 photon per pixel. The most interesting result concerns the low frequencies. When $\bar{n}$ becomes greater than 0.01 the curves present some artifacts near the atmospheric cutoff frequencies ; the visibility functions look like those of a giant star surrouded by a shell. Some astrophysical misinterpretations could occur if the clipping effects are overlooked. The remaining of the curves is not really affected, in particular the first minimum of the Airy function is always very clearly seen and gives the diameter of the

star. We want to emphasize that the interferograms generated by the simulation algorithm are noise free (no photon noise, no additive electronical or thermical noise).
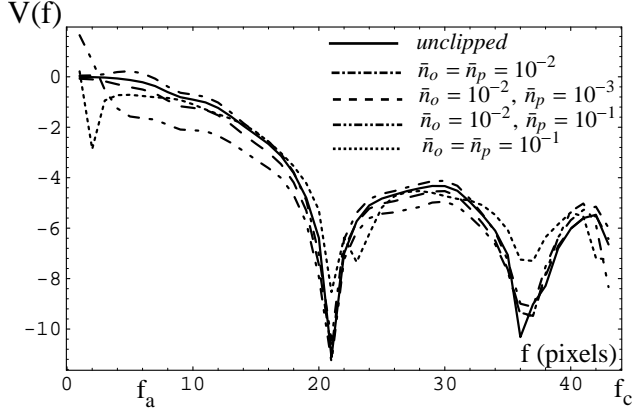
Fig. 8. Plots of the visibility function of a resolved circular object. These curves were computed using the approximation of eq. 10 on simulated speckle interferograms (see text). $\bar{n}_p$ and $\bar{n}_c$ denotes here the mean number of photon per pixel of the psf and of the object respectively. f_c and f_a are the telescope and the atmospheric cutoff frequencies.
.

3.3. Case of a double star

3.3.1. On the AC

The clipped AC and TC are calculated from eq 4 and 6. The probabilities $p_1(0)$, $p_2(0,0;\rho)$ and $p_3(0,0,0;\rho_1,\rho_2)$ are either calculated analytically as describes in section 4 of Paper I or estimated as joint-occurence histograms from a set of images.

For the analytical model, the mathematical fomalism is heavy and we made abundant use of the software *Mathematica* from Wolfram Research. A simplified expression can be given assuming that the speckles are δ-correlated ; the clipped AC of a double star of separation d and intensity ratio β is in this case a sum of three Dirac delta functions weighted by the following terms :

$$\bullet\ C_c(0) \quad = 1 - \frac{1}{(1+\bar{n})(1+\beta\bar{n})}$$

$$\bullet\ C_c(d) \quad = 1 - 2[(1+\bar{n})(1+\beta\bar{n})]^{-1}$$
$$+ [(1+\bar{n})(1+\beta\bar{n})(1+\bar{n}+\beta\bar{n})]^{-1} \tag{17}$$

$$\bullet\ C_c(\rho \neq d) = \left[1 - \frac{1}{(1+\bar{n})(1+\beta\bar{n})}\right]^2$$

The peak corresponding to $\rho = d$ is traditionnaly used to estimate the intensity ratio β of the double star. In
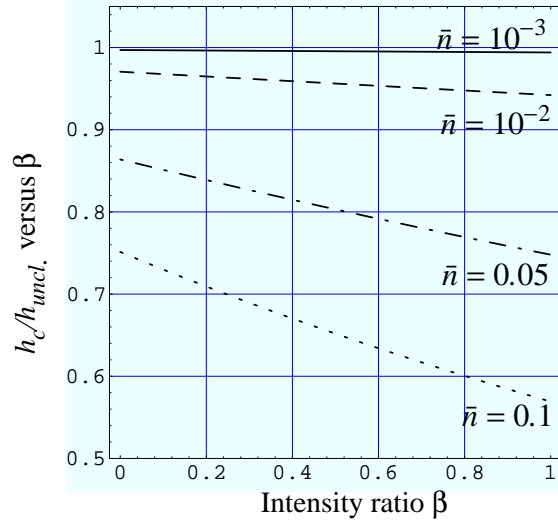
Fig. 9. These curves represent, for a number of photons per pixel varying from 10^{-4} to 0.1, the quantity $h_{\text{clipped}}/h_{\text{unclipped}}$ as a function of the intensity ratio β. h denotes here the height of the secondary peak of the autocorrelation of a double star. As we can see, the clipping decreases the height of the peak. This effect may be of importance if the clipping rate is high : for $\bar{n} = 0.1$ photon/pixel, the intensity ratio can be underestimated by 40 %.

ideal conditions and high light level, the height of the peak (minus the continuous term) is proportionnal to β ; this is no longer the case in clipping conditions. The height h of the peak is equal to :

$$h = C_c(\rho = d) - C_c(\rho \neq d) =$$
$$\bar{n}^2 \beta(1+\bar{n})^{-2}(1+\bar{n}\beta)^{-2}(1+\bar{n}+\bar{n}\beta)^{-1} \tag{18}$$

When $\bar{n} \rightarrow 0$, h tends towards the value $\beta\bar{n}^2$ valid in unclipped conditions. However, some correcting terms must be applied during the measurement of h to obtain a precise estimation of β. Figure 9 shows the variation of the error as a function of $\bar{n}$ and β. It may lead to an underestimation of about 40 % when $\bar{n}$ becomes greater than 0.1 photon per pixel.

The simulation agrees with the above theoretical results. About 1000 images of Vega were processed to simulate a double star with $\beta = 1$ and $\rho = 10$ pixels (about 3 times the size of the speckle). The clipped correlations are plotted on figure 10 ; the secondary peak decreases as $\bar{n}$ increases, and for $\bar{n} = 0.1$ we find $h_{\text{clipped}}/h_{\text{unclipped}} \simeq$ 0.73. The theoretical model give 0.57, but it does not take into account the AC of the long-exposure image, assumed constant in the Gaussian model (space stationnarity).

Another interesting feature concerns the non-linear effect. A simulation of clipped AC of double stars has been made using the analytical model. Figure 11 represents the visibility function of a well resolved star in conditions of
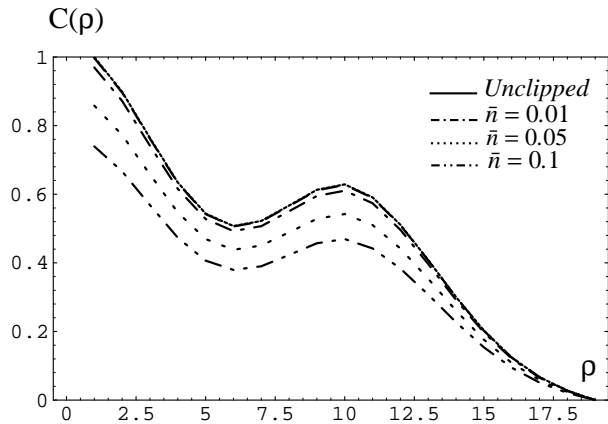
Fig. 10. Functions $\frac{C_c(\rho)-C_c(\rho\gg s)}{C_p(1)-C_p(\rho\gg s)}$ for a double star simulated from images of Vega. The size of the speckle is $s\simeq 3$ pixels, the intensity ratio of the double star is $\beta=1$ and its separation is 10 pixels. The correlation functions have been drawn between $\rho=2$ to 20 (the firsts points are not plotted in order to avoid the Dirac peak at the origin). These curves show the loss of dynamic of the AC and particularly of the peak at $\rho=d$ when the clipping increases.

Fig. 11. Visibility functions of a double star computed using the analytical model with $r(\rho)=2\frac{J_1(\Pi\rho/s)}{\pi\rho/s}$, valid for a circular pupil telescope, s being the size of the speckle ($s=2$ for this run). The parameters of the double star are : intensity ratio $\beta=1$ and separation $d=6$ pixels. The visibility function is estimated by dividing the power spectrum of the double star spekle patterns by the power spectrum of the psf (both are analytic). The full line is for perfect (unclipped) photodetected images, the dashed line is for extremly strong clipped detection ($\bar{n}=10$). f_c is the telescope cutoff frequency.

strong clipping ($\bar{n}=1$) and of no clipping conditions. The fringes relative to the double star seem to prolongate beyond the theoretical cutoff frequency when the clipping is strong. This curious effect may be partly understood if one considers that clipping a function introduces high frequencies in its spectrum.

Another calculus has been made for a close double star. The separation of the binary star was just lower than the size of the speckles, so that the star could not be resolved in normal conditions. The result is illustrated in figure 12. The unclipped AC does not show any duplicate structure, but when the number of photon per pixel becomes greater than 10 or so, we can see that in clipping conditions, the secondary peak appears at ρ equals to the star separation. This may be understood as a consequence of a consequence of the contraction of the point spread AC. Unfortunately this effect is unpracticable for use : firstly because we do not use any more photon-counting detectors at these levels of light, secondly because the ratio $h/C_c(d)\simeq 10^{-4}$ for $\bar{n}=10$; the SNR required to see this effect would then be of the order of 10^4, which corresponds to several hundreds of millions of instantaneous clipped images.

3.3.2. On the TC

The 4-dimensionnal TC $T_c(\rho_1,\rho_2)$ reduces to two dimensions when the vectors ρ_1 and ρ_2 are colinears. For a double star of separation vector $\mathbf{d}$, the TC can be calculated along the $\mathbf{d}$ direction.

As shown by Lohmann et al. (1983), it is possible to obtain a true image of the double star by applying the

object-image convolution relation valid on the TC in absence of clipping :

$$T(\rho_1,\rho_2)=S(\rho_1,\rho_2)*O(\rho_1,\rho_2) \tag{19}$$

where $S(\rho_1,\rho_2)$ is the TC of the psf (traditionnaly estimated on a close reference star) and $O(\rho_1,\rho_2)$ is the double star's triple correlation, which contains several peaks whose relative heights may give the intensity ratio of the stars as illustrated by figure 13.

The starting point for image reconstruction in the triple correlation technique is the TC of the object (or the bispectrum, its Fourier Transform). A review of this technique has been written by Weigelt (1991). The first step before any processing is the compensation of the TC of the PSF (estimated on a reference star nearby) by inverting eq. 19.

In the case of a double star, the intensity ratio may be estimated directly without deconvolution from the TC of the zero-mean signal $T^0(\rho_1,\rho_2)$ (which is also the third-order cumulant). Both functions, calculated with the analytical model, are represented in figure 14. The calculus has been performed by means of eqs. 3.7 and 3.8 of Aime and Aristidi (1991). This calculus gives :

$$\beta=\frac{T(d,0)}{T(d,d)} \tag{20}$$

This expression remains valid for the photodetected speckle patterns ; the photodetected TC $T_p(\rho_1,\rho_2)$ is pro-
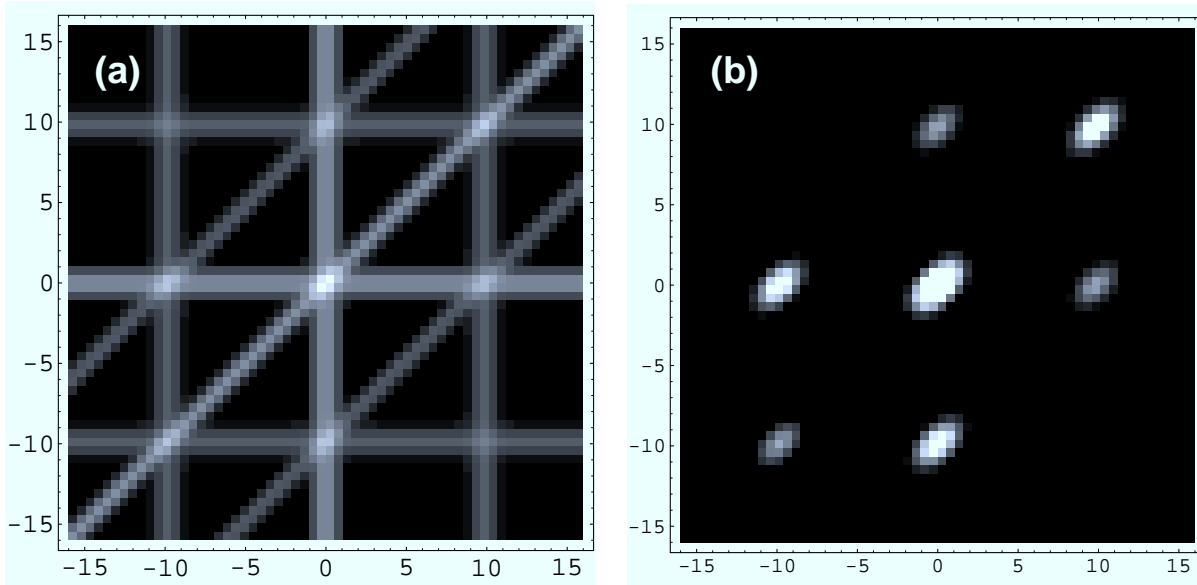
Fig. 14. Comparison of (a) the triple correlation $T(\rho_1, \rho_2)$ of a Gaussian double star speckle pattern at high light level and (b) the triple correlation of the zero-mean speckle patterns $T^0(\rho_1, \rho_2)$ (this quantity is also known as the triple cumulant). The parameters of the double star are : separation $d = 10$, intensity ratio $\beta = 0.3$. This latter function better ressembles the TC of a sum of two Dirac peaks : the vertical, horizontal and diagonal lines have disappeared, making easier the determination of β.
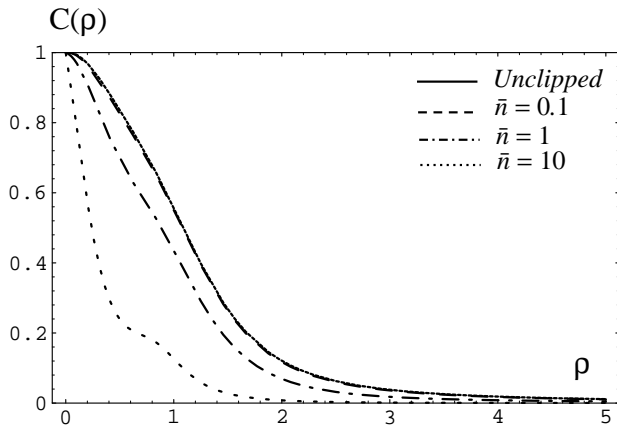
Fig. 12. Clipped AC of a double star speckle pattern computed analytically for a coherence factor $r(\rho) = \exp(-\rho^2/s^2)$. The star separation is 0.8 of the size of the speckle s. The intensity ratio is $\beta = 1$. One can see that althought the star separation is under the theoretical resolution, a strongly clipped detection ($\bar{n} = 10$) makes a second peak appear on the AC at the star separation : this is what we call the "super-resolution effect".

portionnal to the high light TC. The zero-mean photode-tected TC is then :

$$T_p^0(\rho_1, \rho_2) = T_p(\rho_1, \rho_2) + 2\bar{n}^3$$
$$-\bar{n}(C_p(\rho_1) + C_p(\rho_2) + C_p(\rho_2 - \rho_1)) \tag{21}$$
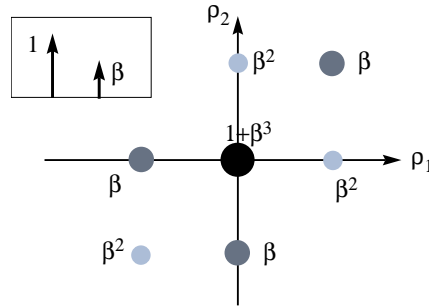
Fig. 13. TC of a double star modelled by the function $\delta(r) + \beta\delta(r - d)$ (as in the frame at the upper left of the figure). The TC is the sum of several peaks whose intensities, written on the scheme, are either β or β^2 ($1 + \beta^3$ at the origin). The intensity ratio β of the stars may be given by the ratio $T(0, d)/T(d, d)$.

This technique has been applied for clipped speckle patterns ; we have computed the quantity

$$T_c^0(\rho_1, \rho_2) = T_c(\rho_1, \rho_2) + 2m_c^3$$
$$-m_c(C_c(\rho_1) + C_c(\rho_2) + C_c(\rho_2 - \rho_1)) \tag{22}$$

Figure 15 shows the ratio $\tilde{\beta} = T_c^0(d, 0)/T_c^0(d, d)$, i.e. the estimator of the intensity ratio β. A good estimation is made when the clipping rate is pretty small ($\bar{n} \leq 10^{-2}$) but where β approaches zero, the ratio has negative values : this is due to the substraction of the correlation terms
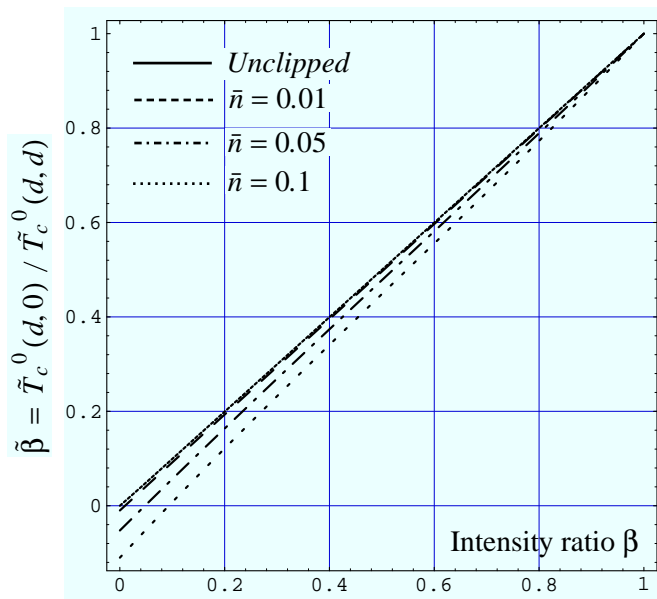
Fig. 15. Variation of $\tilde{\beta}$ (see text) as a function of β for different clipping rates. This concerns the clipped TC's of a double star speckle pattern computed with the analytical model with $r(\rho) = \exp(-\rho^2/s^2)$ and $s = 1$.

in eq. 22. Thus this technique is not applicable in presence of clipping as far as one wants a precise determination of β.

4. Conclusion

We have given in this paper the results of the effects of clipped photon detection in Labeyrie's and Weigelt's speckle techniques (Labeyrie 1970; Weigelt 1977). The problem has been approached both by a theoretical way and a numerical simulation using real data on the bright star Vega. Three examples have been studied : an unresolved point source, a double star and a circular resolved object. For the point source the two approaches have been used and have given comparable results. For the double star the study has been fully theoretical. For the resolved object, the analytical expressions are very complicated and only the simulation has been tested in this case.

The theoretical approach, under the assumption that the complex amplitude of the wave at the focus of the telescope is a circular Gaussian random variable for a point source speckle pattern, allowed us to obtain analytical expressions for the clipped autocorrelation function. The computation was made using either the probability density functions (PDFs) of the speckle pattern, or the moment generating functions (MGFs) as described in Appendix A. The complete formalism, published recently in Paper I, is summarized in the appendix.

The main interest of our study is in the numerical applications, i.e. the computation of the energy transfer functions (ETFs) (two-dimensional Fourier transforms of the autocorrelations for a point source speckle pattern) and the application to structured objects. Under clipping, we have roughly to consider two effects that degrade the ETF : a linear, frequency-independent, loss of energy, and a non-linear deformation of the ETF curve that spreads energy beyond the theoretical cutoff frequency. The two effects are of different magnitude ; for example, the global attenuation of the ETF is already of 20 % when 0.005 % of the pixels are clipped (corresponding to a average number $n = 0.01$ photons per pixel). The non-linear effect requires a higher level of clipping to be visible. For $n = 0.1$ photons per pixel, the rate of non-linearity defined by the percentage of energy transferred beyond the cutoff frequency is only 0.08 %. It becomes significant when n becomes of the order of unity ; this effect is therefore an asymptotic behavior with no real interest in astronomy. Altogether the main conclusion of this study is that the clipping may be neglected when $\bar{n} < 10^{-2}$ photon per pixel.

For a double star speckle pattern, it is interesting to note that the value of the ratio between two components may be misestimated by factors which can reach 40% under strong clipping conditions. This effect may be of importance if one considers the application of binary star measurements to fundamental astronomy (Mc Allister 1988).

The theoretical results are found to be well supported by the numerical simulation performed on more realistic speckles. As we already emphasized it in the body of the paper, the technique which consists in computing first an estimate of the intensity second PDF and then applying a Poisson transform was found of interest from a SNR point of view.

The theoretical study and the numerical simulation were made for single-clipped speckle patterns (number of photons limited to 1). The computation could be easily generalized to the N-clipped case if we had to consider a camera able to detect up to 2, 3 or N photons ; this would be of interest for example whith cameras like electron-bombarded CCD (Cuby 1990) which allow some dynamic in the photoevents.

Appendix A : Analytical expressions of AC and TC for a fully developed speckle pattern

A.1 Use of the moment generating function (MGF) to express the probability of the zero-photon event

The MGF $M(v)$ can be defined as the Laplace transform of the probability density function $P(\Omega)$ (Starck and Woods 1986) :

$$M(v) = \int e^{v.\Omega}\, P(\Omega)\, d\Omega \tag{23}$$

This expression can be generalized to the twofold and threefold MGF :

$$M_2(v_1, v_2; \rho) = \int e^{v_1\Omega_1 + v_2\Omega_2}\, P_2(\Omega_1, \Omega_2; \rho)\, d\Omega_1\, d\Omega_2 \tag{24}$$

$$M_3(v_1, v_2, v_3; \rho_1, \rho_2) = \int e^{v_1 \Omega_1 + v_2 \Omega_2 + v_3 \Omega_3} \tag{25}$$

$$\times P_3(\Omega_1, \Omega_2, \Omega_3; \rho_1, \rho_2)\, d\Omega_1\, d\Omega_2\, d\Omega_3$$

By comparing these expressions with equations 8 and 9 we can write the probabilities $p_1(0)$, $p_2(0,0;\rho)$ and $p_3(0,0,0;\rho_1,\rho_2)$ as functions of the high-light MGF's :

- $p_1(0) = M_1(-\alpha)$

- $p_2(0,0;\rho) = M_2(-\alpha,-\alpha;\rho)$ $\qquad$ (26)

- $p_3(0,0,0;\rho_1,\rho_2) = M_3(-\alpha,-\alpha,-\alpha;\rho_1,\rho_2)$

Substituing relation 26 into 4 and 6 we obtain the expressions of the clipped AC from MGF's :

- $C_c(0) = 1 - M_1(-\alpha)$

$\qquad$ (27)

- $C_c(\rho \neq 0) = 1 - 2M_1(-\alpha) + M_2(-\alpha,-\alpha;\rho)$

and similarly for the clipped TC :

- $T_c(0,0) \quad = 1 - M_1(-\alpha) = C_c(0)$

- $T_c(\rho_1,0) \quad = C_c(\rho_1)$

- $T_c(0,\rho_2) \quad = C_c(\rho_2)$

- $T_c(\rho_1,\rho_1) = C_c(\rho_1)$

$\qquad$ (28)

- $T_c(\rho_1,\rho_2) = 1 - 3M_1(-\alpha) + M_2(-\alpha,-\alpha;\rho_1)$

$\qquad + M_2(-\alpha,-\alpha;\rho_2)$

$\qquad + M_2(-\alpha,-\alpha;\rho_2 - \rho_1)$

$\qquad - M_3(-\alpha,-\alpha,-\alpha;\rho_1,\rho_2)$

A.2 Expression of the MGF of an extended astronomical object speckle pattern

This section is a summary of a paper of Aime and Aristidi (1991) that gives the N-fold characteristic function of an extended object speckle pattern under the hypothesis that the complex amplitude of the wave on the focus of the telescope is Gaussian.

An extended object can be represented by N points weighted by the intensities α_n in the form :

$$O(x) = \sum_{n=1}^{N} \alpha_n\, \delta(x - x_n) \tag{29}$$

For a continuous object, N is the number of sampling pixels. The object can also be represented as a diagonal matrix $\mathbf{D}$ of rank N whose coefficients are the α_n :

$$\mathbf{D} = \begin{bmatrix} \alpha_1 & & & \\ & \alpha_2 & & \\ & & \ddots & \\ & & & \alpha_N \end{bmatrix} \tag{30}$$

We define now the $N \times N$ covariance matrix $\mathbf{R}(\rho)$ of the complex amplitude of the wave at the focus of the telescope, whose coefficient are :

$$\mathbf{R}_{ij}(\rho) = r(x_j - x_i + \rho) = E[\Psi(x_j + \rho)\Psi^*(x_i)] \tag{31}$$

where $\Psi(x)$ is the complex amplitude of the wave in the focal plane for a point-source (it is assumed gaussian in this presentation) ; $r(\rho)$ is then covariance of $\Psi(x)$ (also called "complexe coherence factor" by Goodman (1985)).

The singlefold, twofold and threefold MGF are given as the inverse of the determinant of a matrix :

$$M_1(v) = \det^{-1}(\mathbf{I} - v\mathbf{R}(0)\mathbf{D}) \tag{32}$$

$$M_2(v_1, v_2; \rho) = \det^{-1} \begin{pmatrix} \mathbf{I} - v_1\mathbf{R}(0)\mathbf{D} & -v_2\mathbf{R}(-\rho)\mathbf{D} \\ -v_1\mathbf{R}(\rho) & \mathbf{I} - v_2\mathbf{R}(0)\mathbf{D} \end{pmatrix} \tag{33}$$

$$M_3(v_1, v_2, v_3; \rho_1, \rho_2) = \det^{-1}$$

$$\begin{pmatrix} \mathbf{I} - v_1\mathbf{R}(0)\mathbf{D} & -v_2\mathbf{R}(-\rho_1)\mathbf{D} & -v_3\mathbf{R}(-\rho_2)\mathbf{D} \\ -v_1\mathbf{R}(\rho_1)\mathbf{D} & \mathbf{I} - v_2\mathbf{R}(0)\mathbf{D} & -v_3\mathbf{R}(\rho_1 - \rho_2)\mathbf{D} \\ -v_1\mathbf{R}(\rho_2)\mathbf{D} & -v_2\mathbf{R}(\rho_2 - \rho_1)\mathbf{D} & \mathbf{I} - v_3\mathbf{R}(0)\mathbf{D} \end{pmatrix} \tag{34}$$

where $\mathbf{I}$ is the $N \times N$ unitary matrix.

A.3 Expressions for the point-source speckle pattern

For a point source, the above defined matrix $\mathbf{D}$ reduces to one value representing the intensity of the point-source. The expressions of the MGFs become :

$$M_1(v) = \frac{1}{1 - mv} \tag{35}$$

$$M_2(v_1, v_2; \rho) = \frac{1}{(1 - mv_1)(1 - mv_2) - m^2 v_1 v_2 r^2(\rho)} \tag{36}$$

$$M_3(v_1, v_2, v_3; \rho_1, \rho_2) = [(1 - mv_1)(1 - mv_2)(1 - mv_3)$$

$$- m^3 v_1 v_2 v_3 (r(\rho_2)r(-\rho_1)r(\rho_1 - \rho_2)$$

$$+ r(\rho_1)r(-\rho_2)r(\rho_2 - \rho_1)) \tag{37}$$

$$- m^2 v_1 v_3 (1 - mv_2)r^2(\rho_2) - m^2 v_1 v_2 (1 - mv_3)r^2(\rho_1)$$

$$- m^2 v_2 v_3 (1 - mv_1)r^2(\rho_2 - \rho_1)]^{-1}$$

where m is the mean of the high-light speckle images. By applying equations 26 we obtain after a little algebraic manipulation the expressions of p_1, p_2 and p_3 given in section 2 (equation 12).

References

AIME C., ARISTIDI E., LANTERI H., RICORT G., *SPIE Proc. Mathematical Imaging, Digital Image Synthesis and Inverse Optics*, **1351**, 628 (1990)

AIME C., ARISTIDI E., *J. Opt. Soc. Am. A* **8**, 1434 (1991)

AIME C., ARISTIDI E., *J. Opt. Soc. Am. A* **9**, 1812 (1992)

AIME C., ARISTIDI E., LANTERI H., RICORT G., in *ESO conf. on High resolution imaging by interferometry II*, Garching, October 15, 1991

ARISTIDI E., RICORT G., LANTERI H., AIME C., submitted to *ICO Topical Meeting on Atmospheric, Volume and surface scattering and Propagation*, Florence, 167, 1991

BARAKAT R., *J.Opt. Soc. Am. A* **5**, 1248 (1988)

BLAZIT A., KOECHLIN L., ONETO J.L., *Image Processing Techniques in Astronomy*, ed. C. de Jager and H. Nieuwenhuijzen, Astronomy Institute of Utrech, Netherlands, D.Reidel/Dordrecht (Holland), 79 (1975)

BLAZIT A., Thèse de Doctorat, Université de Nice (1987)

CUBY J.G., *SPIE Proc.* **1235**, 294 (1990)

FOY R., in *9th Santa-Cruz Workshop in Astronomy and Astrophysics*, July 13, 1987, L.B. Robinson, N.Y. : Springer (1987)

FOY R., in *ESO conf. on High resolution imaging by interferometry II*, Garching, October 15, 1991

GOODMAN J.W., *Statistical Optics*, J. Wiley & Sons, N.Y. (1985)

HOFFMANN K.H., WEIGELT G., *J. Opt. Soc. Am. A* **10**, 329 (1993)

HOFFMANN K.H., *Appl. Opt.* **26**, 2011 (1987)

LABEYRIE A., *Astron. Astroph.* **6**, 85 (1970)

LOHMANN A., WEIGELT G., WIRNITZER B., *Appl. Opt.* **22**, 4028 (1983)

MAC ALLISTER H.A., *ESO/NOAO conf on High resolution imaging by interferometry*, 3, Garching, 15-18 March 1988

MARRON J., MORRIS G.M., *J. Opt. Soc. Am. A* **9**, 1403–1410 (1985)

OHTSUBO J., OGIWARA A., *Opt. Comm.* **65**, 73 (1988)

PAPALIOLIOS C., NISENSON P., EBSTEIN S., *Appl. Opt.* **24**, 287 (1985)

PEDERSEN H.M., *J. Opt. Soc. Am. A* **1**, 850 (1984)

PETROV R., KADIRI S., MARTIN F., RICORT G., AIME C., *J. Optics* (Paris) **13**, 331 (1982)

QUIRRENBACH A., in *ESO conf. on High resolution imaging by interferometry II*, Garching, October 15, 1991

RODDIER F., *Physics Reports* **170**, 97, North-Holland (1988)

STARCK H., WOODS J.W., *Probabilities, Random processes and Estimation theory for engineers*, Prentice-Hall, New Jersey (1986)

THIEBAUD E., *Astron. Astroph.* (1994)

WEIGELT G., *Opt. Commun.* **21**, 55 (1977)

WEIGELT G., in *Progress in Optics*, E. Wolf, ed. (Noth-Holland, Amsterdam 1991) **XXIX**, 295 (1991)